

PAPER • OPEN ACCESS

Study on airflow characteristics of rear wing of F1 car

To cite this article: A R S Azmi *et al* 2017 *IOP Conf. Ser.: Mater. Sci. Eng.* **243** 012030

View the [article online](#) for updates and enhancements.

You may also like

- [Aerodynamic comparison of a butterfly-like flapping wing-body model and a revolving-wing model](#)
Kosuke Suzuki and Masato Yoshino
- [Experimental Study on the Propulsion Performance of the M-shape flapping wing's bending angle](#)
Jingxian Chen, Xiaofang Nie and Ximing Zhou
- [Design optimization and experimental study of a novel mechanism for a hover-able bionic flapping-wing micro air vehicle](#)
Huichao Deng, Shengjie Xiao, Binxiao Huang et al.



The Electrochemical Society
Advancing solid state & electrochemical science & technology

241st ECS Meeting

Vancouver, BC, Canada. May 29 – June 2, 2022



ECS Plenary Lecture featuring
Prof. Jeff Dahn,
Dalhousie University



Register now!



Study on airflow characteristics of rear wing of F1 car

A R S Azmi¹, A Sapit¹, A N Mohammed¹, M A Razali¹, A Sadikin¹, N Nordin¹

¹Flow Analysis, Simulation and Turbulence Research Group, Faculty of Mechanical and Manufacturing Engineering, Universiti Tun Hussein Onn Malaysia, Johor, Malaysia

E-mail: ar.salami94@gmail.com

Abstract. The paper aims to investigate CFD simulation is carried out to investigate the airflow along the rear wing of F1 car with Reynold number of 3×10^6 and velocity, $u = 43.82204$ m/s. The analysis was done using 2-D model consists of main plane and flap wing, combined together to form rear wing module. Both of the aerofoil is placed inside a box of 350mm long and 220mm height according to regulation set up by FIA. The parameters for this study is the thickness and the chord length of the flap wing aerofoil. The simulations were performed by using FLUENT solver and k- ϵ -omega model. The wind speed is set up to 43 m/s that is the average speed of F1 car when cornering. This study uses NACA 2408, 2412, and 2415 for the flap wing and BE50 for the main plane. Each cases being simulated with a gap between the aerofoil of 10mm and 50mm when the DRS is activated. Grid independence test and validation was conduct to make sure the result obtained is acceptable. The goal of this study is to investigate aerodynamic behavior of airflow around the rear wing as well as to see how the thickness and the chord length of flap wing influence the airflow at the rear wing. The results show that increasing in thickness of the flap wing aerofoil will decreases the downforce. The results also show that although the short flap wing generate lower downforce than the big flap wing, but the drag force can be significantly reduced as the short flap wing has more change in angle of attack when it is activated. Therefore, the type of aerofoil for the rear wing should be decided according to the circuit track so that it can be fully optimized.

1. Introduction

Aerofoil in motorsports are called wings where it can generate high downforce by having a high angle of attack, therefore increasing the drag of the aerofoil. Daniel Bernoulli deduced a formula proving that the total energy in steadily flowing fluid system is a constant along the flow path. An increase on the fluid's speed will resulting in decrease in its pressure. Adding up the pressure variation times the area around the entire body determines the aerodynamic force on the body [1].

Aerofoils are mostly designed with more thickness on the lower side. As downforce generating, the lower airstream is slightly reduced in surface, hence increasing the flow speed and decreasing the pressure. On top of the wing, the airspeed is lower, thus the pressure difference will generate a downward force on the wing. More specifically, the shape of the wing will turn air upwards and change its velocity [1].

Drag Reduction System (DRS) is a new development that have been introduced in F1 in the year of 2011. The DRS is a system where the flap wing will be opened up when it is activated for overtaking aid. Drivers are free to activate the DRS as they wish within the designated DRS zones during practice and qualifying. However, if the DRS is disabled at any point during Q1, Q2 or Q3, it will remain disabled for the remainder of the relevant period. The rule for activating the DRS is the driver only



may activate it when they are within one second of the car in front at the DRS detection point. The DRS will automatically be disabled that is resetting the rear wing flap to its original position the first time the driver uses the brakes after activation [2].

Computational Fluid Dynamic (CFD) is a sophisticated computationally-based design and analysis technique that uses computational technology that enables researcher to study the dynamics of things that flow. Using CFD, a computational model that represents a system or device can be build. Then the fluid flow physics and chemistry can be applied to this virtual prototype and the software will output a prediction of the fluid dynamics and related physical phenomena. Besides, CFD software can give the power to simulate flows of gases and liquids, heat and mass transfer, moving bodies, multiphase physics, chemical reaction, fluid-structure interaction and acoustics through computer modelling. A lot of time can be save that normally need to use for building prototype by using CFD [3].

CFD is broadly used in the racing industry to predict the downforce and the drag of race cars that would experience at high velocities. CFD provides numerical solutions to the governing equations of fluid dynamics throughout the desired flow region. It takes into account for complex problems to be solved without losing the integrity of the problem due to over-simplification. It is this ability to solve large problems that makes CFD an efficient tool for the automotive industry. CFD allows engineers to examine the airflow over an automobile or a particular part such as a wing or hood, and see the aerodynamic effect of changing the geometry of any particular area of the vehicle [4].

Therefore, simulation has been done to see how the thickness and chord length of the flap wing influence the drag force, downforce, lift and drag coefficient of the rear wing.

2. Methodology

2.1. Rear wing design

There are a total of 12 models that were simulated for three different thickness of NACA 2408, 2412, and 2415 for the flap wing when it is close at 10mm gap and 50mm when it is activated. The difference in length of the flap wing also being tested namely big and short flap wing. The simulations has been ran using FLUENT solver with initially compared with three different types of turbulences model. The geometry of all 12 models were modeled in SolidWork software before imported into ANSYS. The geometry of the models for big flap is shown in the Table 1 while the Table 2 shows the one with short flap wing. In the case of big flap, the chord length for the main plane is 250mm while for the flap wing is 175mm, and for the case of short flap, the chord length of the main plane is 290mm while the flap wing is 120mm.

Table 1. Rear Wing Model with Big Flap Wing













NACA	Model	
	10mm	50mm
2408		
2412		
2415		

Table 2. Rear Wing Model with Short Flap Wing

NACA	Model	
	10mm	50mm
2408		
2412		
2415		

2.2. Grid independence test (GIT)

Grid independence test has been conducted to see the accuracy of the mesh and the result obtained. The test has been done with three grids which started with coarse, medium, and then fine meshing. The medium is the refinement of coarse meshing and the fine is the refinement of the medium meshing. The element, nodes, and the result of lift coefficient value of those three grids are presented in the Table 3 below.

Table 3. NACA 2415 GIT

Grid type	Nodes	Elements	Iteration to converged	Lift coefficient, c_l
Coarse	22899	22595	174	0.188771
Medium	46238	45760	211	0.195898
Fine	98762	98184	436	0.204577

2.3. Validation

In term of validation of the result, the single aerofoil of NACA 2415 have been chosen to compare the numerical result that have been ran using CFD FLUENT with the experimental result. The reason of validation with only single aerofoil was because there is hardly any experimental data for the rear wing of F1 cars as they are a closely guarded secret. Therefore, a single aerofoil has been chosen for validation before conducting with the real cases. The validation of the data has been conducted to make sure that the data of this numerical research is on the right track by having small margin error when compared to the experimental result. The experimental data that had been compared with the numerical data was obtained from a book produced by the director of NASA [5]. The experimental data of the NACA 2415 is shown in the Figure 1 and Table 4 below.

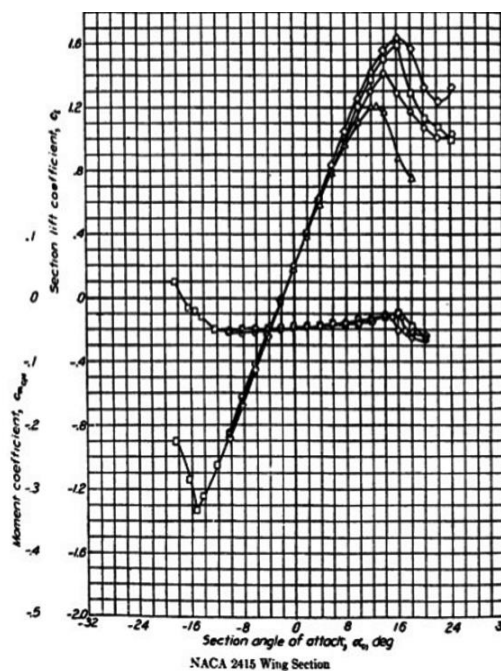


Figure 1. NACA 2415 experimental result

Table 4. Experimental data of NACA 2415 at $Re=3 \times 10^6$

Experimental lift coefficient, c_l	Experimental angle of attack, α
0.09193992713054255	-1.0179211469534124
0.1616102372700614	-0.3154121863799304
0.200682992	0
0.23620367901892836	0.28673835125447766
0.2860037323380431	0.8888888888888857

The Table 4 shows the experimental data of NACA 2415 with Reynolds number of 3×10^6 . The numerical simulation of the NACA 2415 has been conducted at an angle of attack of 0 degree with three different types of turbulent models which are k-epsilon, k-omega, and k-kl-omega transition. The result was then compared with the 0 degree angle of attack experimental data which is 0.200682992. The comparison of the data is shown in the Table 5.

Table 5. Comparison of numerical and experimental data

Turbulence model	Experimental lift coefficient, c_l	Numerical lift coefficient, c_l	Error percentage
K-epsilon	0.200682992	0.18822	6.21
K-omega	0.200682992	0.21998	9.62
K-Kl- ω	0.200682992	0.20458	1.94

From the Table 5, k-kl- ω turbulence model has the smallest error percentage of 1.94. For airfoils operating in the Re range of 10^6 , the adverse pressure gradient is eliminated by turbulent flow at transition thus preventing separation. An increase in Re induces turbulence in the boundary layer, imparting high energy to oppose separation. From the result it can be seen that k-kl- ω is more reliable for predicting separation bubble formation, growth and reattachment for this cases. Therefore, k-kl- ω has been used to calculate all the cases.

3. Results analysis and discussion

3.1. Contour results

The pressure and velocity contour for rear wing of F1 car have been extracted from the post-processing for all models. The pressure and the velocity contour of both when the wings is at 10mm and 50mm are presented in the Table 6 and Table 7.

Table 6. Pressure contour for all models

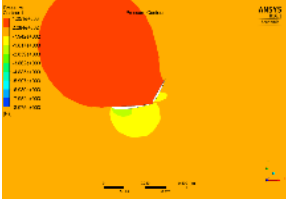
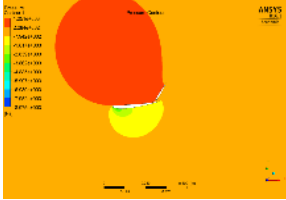
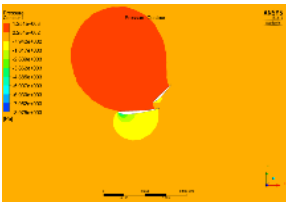
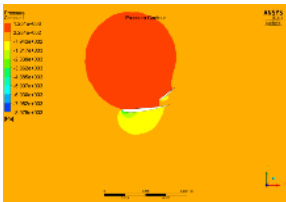
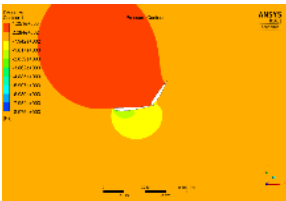
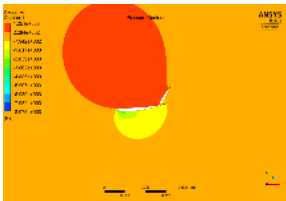
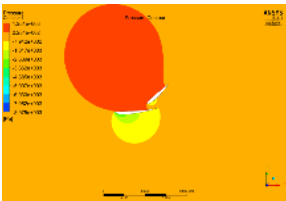
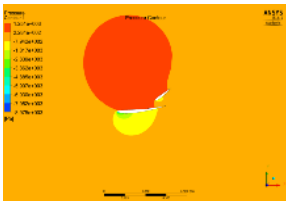
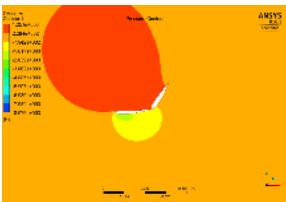
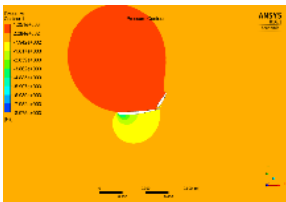

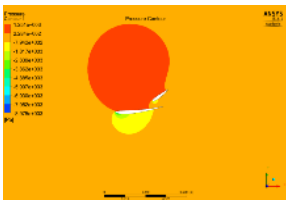
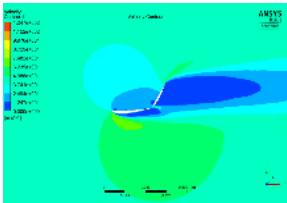
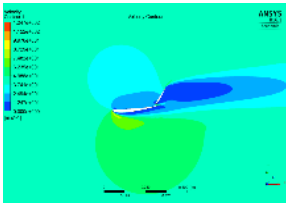
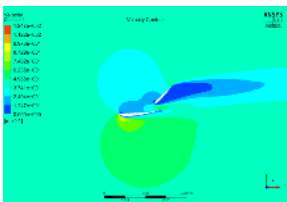
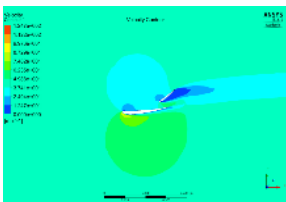
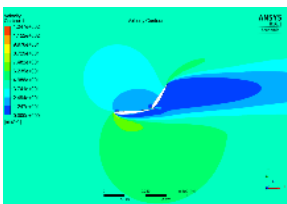
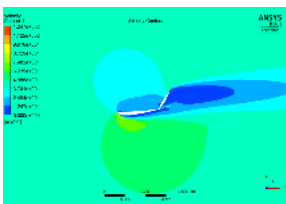
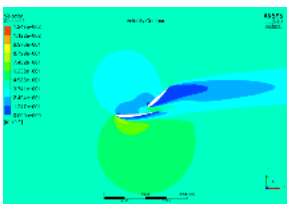
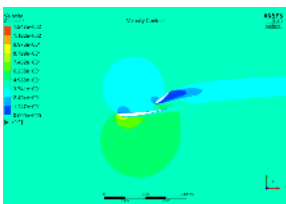
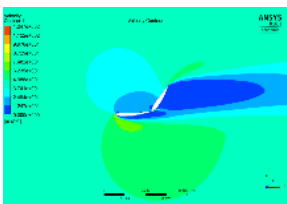
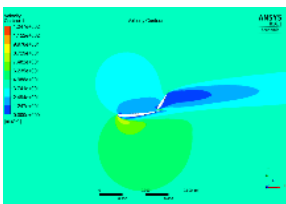
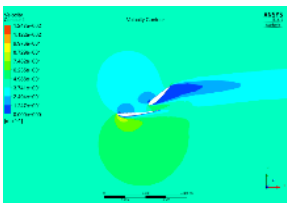
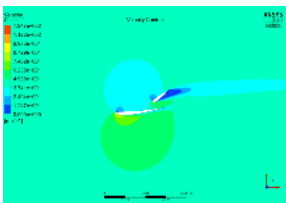
NACA	Gap (mm)	Pressure contour	
		Big flap	Short flap
2408	10		
	50		
2412	10		
	50		
2415	10		
	50		

Table 7. Velocity contour for all models

NACA	Gap (mm)	Velocity contour	
		Big flap	Short flap
2408	10		
	50		
2412	10		
	50		
2415	10		
	50		

From the Table 6 and Table 7, it can be seen that the pressure on the upper side of the aerofoil have larger pressure than the lower side of the aerofoil due to the high velocity at the lower side of the aerofoil. The Bernoulli's principle stated that by increasing in the velocity will be resulting in the decreases in pressure. Therefore, a downward force was generated by the wings. It also can be seen that by having less thickness of aerofoil on the flap wing will generate more pressure on the rear wing thus will increase the downforce of the F1 car. When the Drag Reduction System (DRS) is activated, the pressure generated by the wings was reduce therefore resulting in increasing of velocity. This is because, when the flap wing was open with a gap of 50mm, it will allow more air to passed through and decreased the drag compared to the one with a gap of 10mm where a lot more surface exposed to stagnation.

3.2. Pressure against distance

In order to get clearer view of pressure distribution for all of the cases, the graph of pressure distribution versus distance along x-axis were presented in the Table 8 and Table 9 below. Each figure has two shape of pressure because there were two aerofoil involves. The bigger one represent the main plane of the rear wing while the smaller one represent the flap wing. The point for each surfaces is shown in The Figure 2 below.

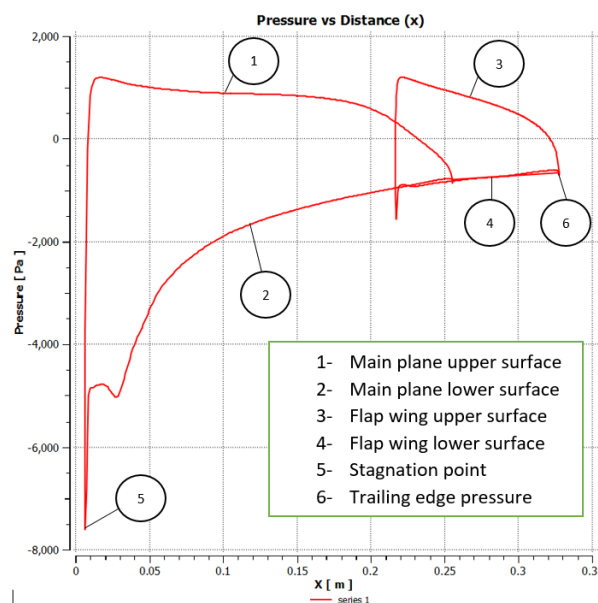


Figure 2. Pressure vs distance graph

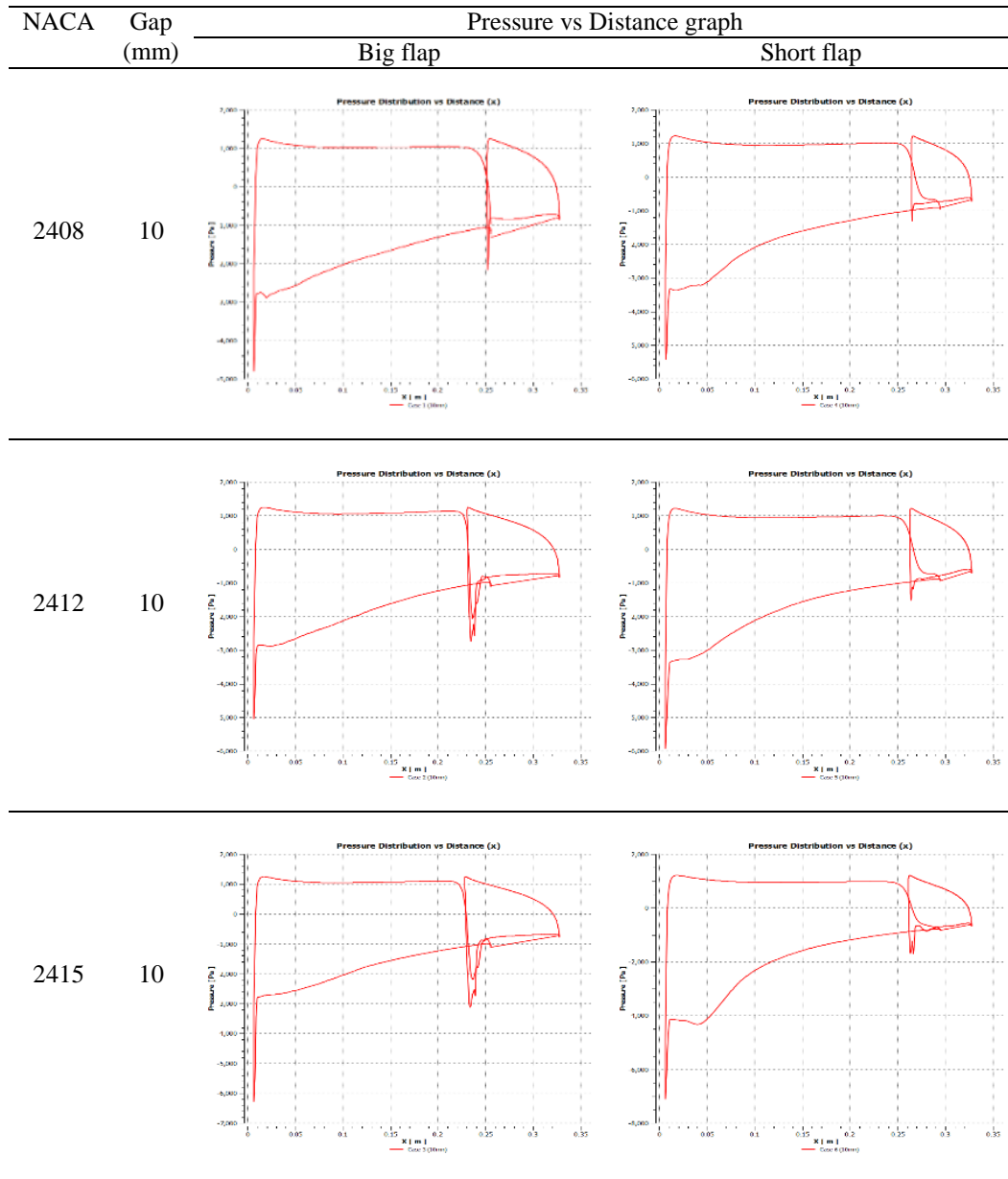
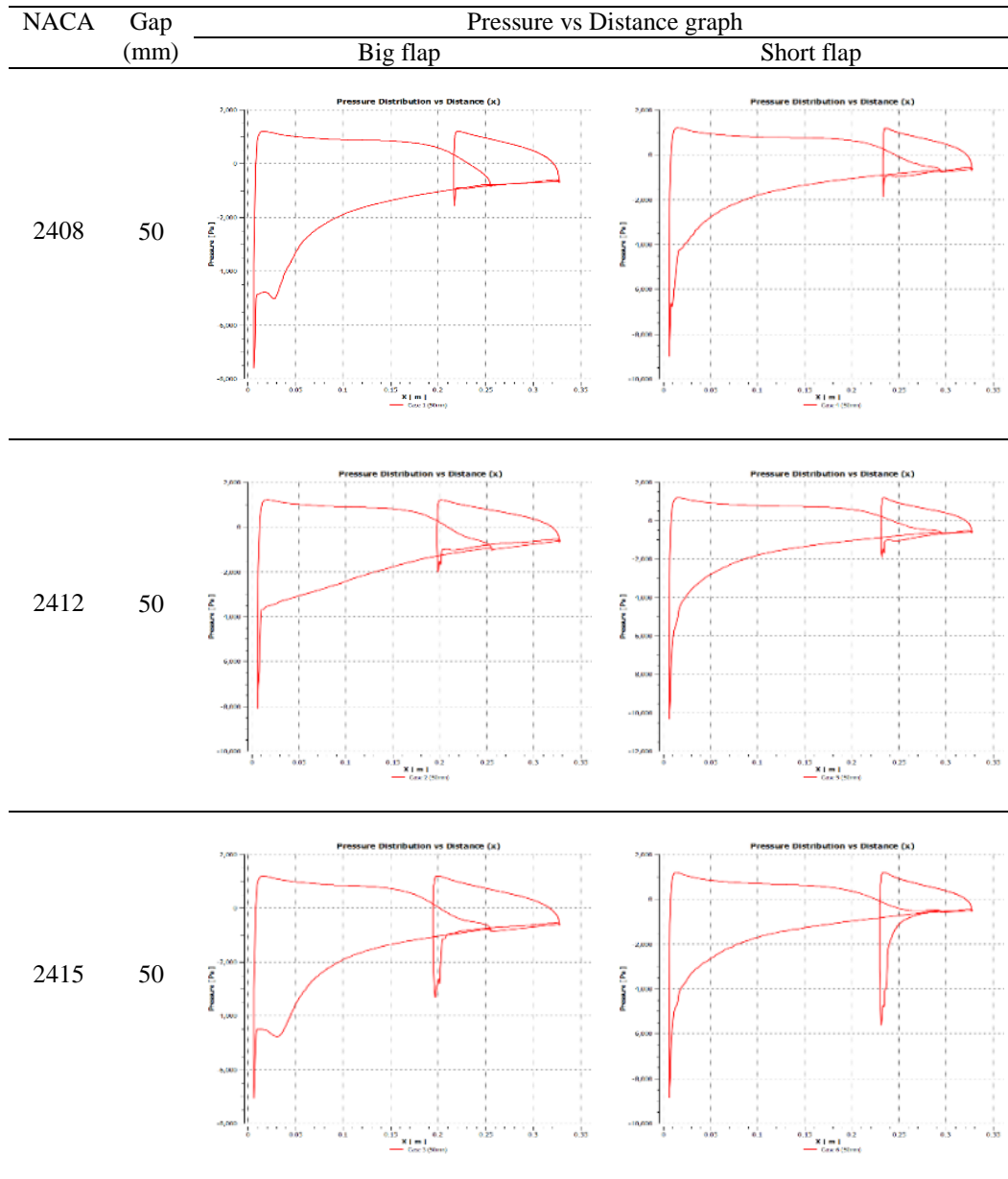
Table 8. Velocity contour for models with 10mm gap

Table 9. Velocity contour for models with 50mm gap

From the Table 8 and Table 9, we can see that the pressure on the lower surface is lower than the upper surface thus causing the higher pressure to press the lower pressure resulting in downward force. As the distance is increasing, the pressure is decreasing as it reached the trailing edge. The point 5 and point 6 is the stagnation point and the trailing edge pressure where it is occurred for both on the main plane and on the flap wing. The stagnation for the flap wing is higher when it is at 10mm because more surface area exposed to the wind.

3.3. Drag and lift forces

Drag and down force is an important factor that need to be taken into consideration when designing rear wing of F1 car. The results for the drag coefficient and force, lift coefficient and force, and the lift over drag ratio of the overall rear wing is presented in the Table 10 below.

Table 10. Forces and coefficient of all cases

Type of flap wing	NACA	Wing's gap (mm)	Drag force (N)	Down force (N)	Drag coefficient, Cd	Lift coefficient, Cl	L/D
Big	2408	10	246.73195	924.27946	0.2098	0.7859	3.746
		50	141.03082	865.79765	0.1199	0.7291	6.139
	2412	10	245.69891	872.072	0.2089	0.7415	3.549
		50	159.00314	849.73987	0.1352	0.7225	5.344
	2415	10	230.13479	857.43091	0.1957	0.7361	3.726
		50	129.17991	839.99689	0.10813	0.7142	6.503
Short	2408	10	176.06802	839.8714	0.1497	0.7141	4.77
		50	84.633378	799.84627	0.07119	0.6801	9.451
	2412	10	168.87273	838.98505	0.1436	0.7133	4.968
		50	67.08332	791.56129	0.057	0.673	11.8
	2415	10	145.51319	819.11694	0.1237	0.6964	5.629
		50	51.32626	745.62411	0.0436	0.634	14.816

From the Table 10, the NACA 2415 with short flap wing has the highest L/D for both gap of 10mm and 50mm. This shows that the NACA 2415 is the best model when compared to the other models as it generates more downforce in addition to less drag force. The yellow colour indicates the highest value for wings with gap of 10mm while the green colour indicates the highest value for 50mm wing's gap.

4. Conclusion

From the simulation using k- ϵ -omega turbulence model, it can be seen that the drag force, downward force, lift coefficient, and drag coefficient have been obtained. The pressure and velocity for all cases are presented in the form of contours and graphs. From Table 6 and 7, it can be seen that the thickness of the aerofoil for the flap wing influences the down force and the drag force of the rear wing module (combination of main wing and flap wing). Increases of thickness will decreases the downforce and drag force produced by the rear wing. From all the obtain results, it can be concluded that the short

flap wing is favourable when facing a circuit that have more straight track. Although the short flap wing produced lower downforce when compared to the big flap wing, but when the DRS is activated, it can reduce the drag force significantly therefore will increases the speed of the F1 car.

References

- [1] Katz J 2006 Aerodynamics of race cars *Annu. Rev. Fluid Mech.* **38** 27-63
<https://doi.org/10.1146/annurev.fluid.38.050304.092016>
- [2] Formula 1® - The Official F1® Website 2017 Drag Reduction System. Retrieved from:
https://www.formula1.com/en/championship/inside-f1/rules-regs/Drag_Reduction_System.html
- [3] Versteeg H K and Malalasekera W 1995 *An introduction to computationnal Fluid Dynamics, The finite volume control, éd* (New York: Longman Scientific and Technical, John Wiley & Sons Inc)
- [4] Chandra S 2011 CFD Analysis of PACE Formula-1 Car *Comput. Aided Des. Appl.* PACE **1** 1-14
<https://doi.org/10.3722/cadaps.2011.PACE.1-14>
- [5] Abbott I H and Von Doenhoff A E 1959 *Theory of wing sections: Including a summary of airfoil data* (Mineola, New York: Dover publication)